Wear 305 (2013) 238–247

Contents lists available at ScienceDirect

Wear

journal homepage: www.elsevier.com/locate/wear

Tribological behavior of components for radial piston hydraulic motors: Bench tests, failure analysis and laboratory dry sliding tests

L. Ceschini, A. Marconi, C. Martini*, A. Morri

Department of Industrial Engineering (DIN), University of Bologna, Via Risorgimento 4, 40136 Bologna, Italy

ARTICLE INFO

Article history:
Received 20 December 2012
Received in revised form
13 June 2013
Accepted 17 June 2013
Available online 26 June 2013

Keywords:
Sliding wear
Two-body abrasion
Carburized steel
Thermal spray coatings
Electron microscopy

ABSTRACT

Bench tests and laboratory dry sliding tests were carried out on components for radial piston hydraulic motors involved in a boundary-lubricated sliding contact, with the aim of investigating the tribological behavior and improve their durability. Failure analysis of real components after bench tests (carried out on a rotating shaft, consisting of a quenched and tempered 36CrNiMo4 steel, coated by a Ni7Al layer deposited by Air Flame Spray, sliding against a carburized E470 steel contacting element) identified the main wear mechanism as two-body abrasion, due to hard particles detached from the AFS coating which induce severe plastic deformation on both the carburized steel contacting element and on the soft Ni-based matrix of the coating on the rotating shaft. The same wear mechanism was reproduced also in laboratory dry sliding tests, carried out on a block-on-ring tribometer under dry sliding conditions. Laboratory dry sliding tests allowed the investigation of the influence of normal load and sliding distance on friction and wear behavior of the tribological system under investigation.

1. Introduction

Radial piston hydraulic motors, which transmit force to the driving shaft by means of a pressurized oil column, are widely used in applications where low speed and high torque are required [1,2]. These motors include several moving components with sliding and rolling contacts [3], which may be improved in terms of tribological behaviour. Specifically, steel components such as the rotating shaft undergo wear, due to sliding against the telescopic cylinders which contain the oil column, and the formation of wear marks on both contacting surfaces leads to oil leakage and decrease of the rotating speed. The durability of the motor can therefore be improved by appropriate surface modification treatments, such as the deposition of thermal spray coatings for adhesive/abrasive wear applications [4] on the rotating shaft and/or thermochemical treatments, such as carburizing for the steel counterface [5].

The present work aims at the selection of candidate surface treatments and materials for the improvement of the tribological behavior of the rotating shaft/telescopic cylinder system. To this aim, the main wear mechanisms involved during sliding on both rotating shafts and contacting elements, belonging to the telescopic cylinders, need to be fully investigated both by bench tests and laboratory dry sliding tests. Particular attention, therefore, will be devoted to reproducing the same wear mechanisms identified by failure analyses on the components after bench tests also in laboratory tests, which allow a deeper evaluation of the influence of sliding conditions (normal load and distance) on the tribological behavior of the system.

2. Materials and methods

2.1. Tribological system

The principle of hydraulic motors under investigation is to transmit force to the driving shaft by means of a pressurized oil column, without any connecting rods, pistons, pads and pins. The hydraulic fluid is sealed between the spherical surface of the cylinder head and the rotating shaft, which undergo relative sliding motion (Fig. 1). The tribological system under investigation therefore consists of a rotating shaft, as the main body, and a contacting element, which belongs to the telescopic cylinder, as the counterfacing body. The contacting element cannot be further described due to confidentiality reasons. The hydraulic fluid (a standard mineral hydraulic oil) enters the contact area between the two contacting bodies, however the system is mostly in boundary lubrication conditions. The rotating shaft is made of the quenched and tempered 36CrNiMo4 steel (according to EN 10083 [6]), sand blasted then coated with an Air Flame Sprayed (AFS) Ni-based layer, while the contacting element consists of steel for seamless circular tubes E 470 (UNI EN 10297-1 [7]), carburized to a nominal case depth of 800 ± 150 μm (Cmt8 according to UNI 5381 standard [8]).

* Corresponding author. Tel.: +39 51 2093464; fax: +39 51 2093467.
E-mail address: carla.martini@unibo.it (C. Martini).

0043-1648/$ - see front matter © 2013 Elsevier B.V. All rights reserved.
http://dx.doi.org/10.1016/j.wear.2013.06.012

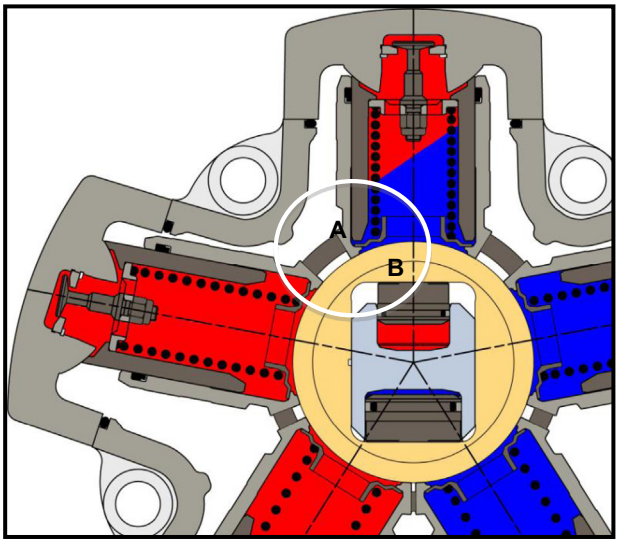

Fig. 1. Schematic drawing of the hydraulic motor under investigation. A circle surrounds the contacting element of the telescopic cylinders (A) and the rotating shaft (B).

Nominal material compositions for the steels and the Ni-based powders (size ranging from 45 to 125 μm) for the deposition of the AFS coating are reported in Tables 1–3, together with indications about the surface treatments/coating on the two contacting bodies. The volume percentage of retained austenite in carburized E470 steel and the phase constitution of the AFS coating was determined by XRD, performing θ–2θ scans with a Co or a Cu K_α radiation source, respectively. The residual porosity in the AFS coating was determined by image analysis (Image Pro Plus software v. 5.1) of micrographs at 400× magnification, on samples prepared and analyzed according to the procedure described in [9].

2.2. Bench tests

Bench tests were performed on real hydraulic motors in representative in-service conditions: namely, the influence of sliding distance (S) on wear was taken into account by setting two different S values: 5000 m (short-run tests, SR) and 20,000 m (long-run tests, LR), keeping constant the settings for oil supply pressure (200 bar) and sliding speed (130 rpm). At the end of the tests, the motors were disassembled and failure analysis of worn components was carried out.

2.3. Failure analysis

Failure analysis was carried out by morphological observation of worn surfaces by optical microscopy (OM), 3D-digital microscopy and scanning electron microscopy (SEM) with an Energy Dispersive Spectroscopy (EDS) microprobe, so as to identify the dominant wear mechanisms. Metallographic analysis of the materials in contact (after conventional metallographic preparation of mounted and polished samples) was also carried out by the same techniques, before and after bench tests. Finally, Vickers microhardness tests were used to check both the surface hardness and cross-section hardness profiles.

2.4. Tribological testing (lab-scale dry sliding tests)

Tribological tests were also carried out on the laboratory scale, in conditions selected for reproducing the real tribosystem, in which the dominant wear mechanism was identified by failure analysis on worn components from bench tests. The aim of these tests was the evaluation of the influence of sliding conditions, namely distance and normal load, on the friction and wear behavior. Non-lubricated conditions were selected for laboratory tests, because only boundary lubrication can be available during in-service condition for the tribosystem under investigation. Dry sliding tests were therefore carried out on a slider-on-cylinder tribometer (block-on-ring contact geometry), described in more detail elsewhere [10]. In this test, carburized E470 steel specimens ($5 \times 5 \times 70$ mm^3) were used as stationary sliders, whilst the rotating cylinder (40 mm diameter) was a quenched and tempered 36CrNiMo4 steel, coated with a Ni-based AFS coating (both with a surface roughness R_a lower than 0.20 μm and a surface hardness of 700 HV_1 and 480 ± 70 $HV_{0.3}$, respectively, as in the case of real tribocomponents, which are described in Section 3.1). Sliding tests were carried out at ambient conditions of temperature and humidity, at a sliding speed of 1.4 m/s, over sliding distances of 5, 10 and 20 km, under normal loads ranging from 10 to 40 N. During the tests, friction force and vertical displacement, which is related to total wear (i.e. cumulative wear of both stationary slider and rotating cylinder), were continuously measured by means of a bending load cell and a linear variable differential displacement transducer (LVDT), respectively. Friction and wear data were recorded as a function of sliding distance. After the tests, wear scar depths and widths on sliders were evaluated by stylus profilometry. Wear volumes were calculated according to ASTM G77-05 [11]. Wear scars on sliders and wear debris were characterized by SEM and EDS, whilst the morphology of the wear scars on rotating cylinders was non-destructively characterized by 3D-digital microscopy, in order to identify the dominant wear mechanisms.

3. Results and discussion

3.1. Microstructural characterization of the contacting bodies

The contacting element, consisting of carburized E470 steel, showed a martensitic microstructure in the case hardened layer (Fig. 2a). The retained austenite volume percentage, determined by XRD, ranges from 9 to 15 vol%, which is acceptable for such a component in this kind of application. The Vickers micro-hardness profile in cross section showed a surface hardness of about 750 HV_1 and a case hardened depth of about 0.45 mm for both the as-supplied and the worn component (Fig. 2b). The decrease of case hardened depth (by comparison to the standard value for Cmt8, as reported in Section 2.1) is due to the grinding operation, routinely carried out before servicing the component.

The air flame-sprayed (AFS) coating deposited on the rotating shaft is shown in Fig. 3 (cross section in Fig. 3a; free surface, after grinding, in Fig. 3b; X-ray EDS map of the free surface in Fig. 3c). The cross section in Fig. 3a shows the typical layered structure of thermal spray coatings, with partially coalesced splats, interlamellar pores and rounded, unmelted particles (with size comparable to that of the original powders, see Section 2.1). Pores and cracks are visible also on the as-deposited free surface (Fig. 3b), possibly favoring lubricant retention during sliding. The black rounded pores are artifacts due to metallographic preparation (i.e. detachment of unmelted particles), whilst "half-penny" shaped pores (curved side on top and the straight side on bottom) were probably due to the expansion of trapped air when the impacting particles were still molten [12]. The overall porosity of the coating evaluated by image analysis was 6 ± 1%.

The average thickness of the AFS coating was 310 ± 15 μm. Surface hardness was 470 ± 100 $HV_{0.03}$ (the deviation from the average being rather high, due to the non-homogeneous